ELSEVIER

Physica C 364–365 (2001) 386–391

PHYSICA C

www.elsevier.com/locate/physc

Electron magnetic resonance imaging of the Fermi surface of Sr_2RuO_4

C. Palassis [a], M.M. Mola [a], S. Hill [a,*], J.S. Brooks [b], Y. Maeno [c,d], Z.Q. Mao [c,d]

[a] *Department of Physics, Montana State University, Bozeman, MT 59717, USA*
[b] *Department of Physics and the NHMFL, Florida State University, Tallahassee, FL 32310, USA*
[c] *Department of Physics, University of Kyoto, Kyoto 606-8502, Japan*
[d] *CREST-JST, Kawaguchi, Saitama 332-0012, Japan*

Abstract

We have carried out detailed angle dependent studies of the normal state microwave (40–112 GHz) magneto-conductivity of several single crystal samples of the perovskite superconductor Sr_2RuO_4. As previously reported [Phys. Rev. Lett. 84 (2000) 3374], we observe a series of resonant absorptions which we attribute to cyclotron resonance of quasiparticles belonging to the three well-known Fermi surfaces for this material. From the angle dependence, we confirm the two-dimensional character of these resonances, i.e. the cyclotron frequencies scale as the inverse cosine of the angle between the magnetic field and the normal to the conducting layers. Furthermore, by performing measurements on several samples, and in different electromagnetic field configurations, we are able to couple to different cyclotron modes (+ harmonics) which derive from deformations (warpings) of the Fermi surfaces from perfect cylinders. These mode couplings will be discussed in the light of recent angle dependent de Haas–van Alphen measurements. © 2001 Elsevier Science B.V. All rights reserved.

Keywords: Cyclotron resonance; Sr_2RuO_4; Triplet superconductor; Effective mass

1. Introduction

One of the more fascinating problems in condensed matter physics today concerns the nature of the superconducting state in Sr_2RuO_4 [1]. For almost three decades, it has been known that a triplet superfluid state arises in ^{3}He which is mediated by ferromagnetic spin fluctuations with a momentum distribution peaked at $\mathbf{q} = 0$ [2]. Recent NMR [3] and μSR [4] experiments have provided convincing evidence for a triplet superconducting state in Sr_2RuO_4. Meanwhile, neutron experiments provide no evidence for the expected $\mathbf{q} = 0$ spin-fluctuation peak [5]; instead, significant peaks at $\mathbf{q}_0 = (\pm 2\pi/3, \pm 2\pi/3)$ are observed, suggesting that antiferromagnetic (AF) spin fluctuations may be responsible for the Cooper pairing in Sr_2RuO_4. These experimental observations apparently contradict one another, since a singlet superconducting state is usually expected to result from an AF spin-fluctuation mediated pairing mechanism, as is now thought to be the case in the high-T_c cuprates [6]. To circumvent this

* Corresponding author. Tel.: +1-406-994-7175; fax: +1-406-994-4452.
E-mail address: hill@physics.montana.edu (S. Hill).

0921-4534/01/$ - see front matter © 2001 Elsevier Science B.V. All rights reserved.
PII: S0921-4534(01)00804-8

paradox, a number of recent theoretical works have demonstrated that, under certain conditions, finite **q** charge and spin fluctuations can give rise to a triplet state [7,8]. What is more, the conditions most favorable for the triplet case depend very sensitively on the nesting characteristics of the underlying electronic bands (Fermi surface – FS). Thus, a detailed knowledge of the FS topography of Sr_2RuO_4 is essential before the nature of its superconducting state can be completely resolved.

Angle-dependent magnetoresistance oscillation (AMRO) measurements [9], angle-resolved photoemission spectroscopy [10], and local density approximation (LDA) calculations [11] provide important information regarding the cross-sectional shapes of the three approximately cylindrical FSs for Sr_2RuO_4. However, these methods do not enable truly 3D topographic FS imaging. This has important consequences as far as nesting is concerned, since it is known that a weak *c*-axis dispersion causes significant periodic deformations (warpings) of the FSs (on the order of 1%) as a function of the *c*-axis momentum (see Fig. 1a); these deformations will, in turn, affect the FS nesting characteristics.

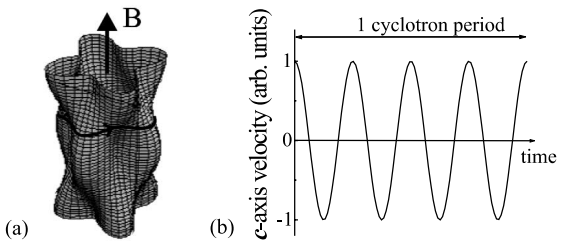

Fig. 1. (a) Schematic representation of a warped quasi-two-dimensional Fermi cylinder; for Sr_2RuO_4, the *c*-axis is parallel to the cylinder axis. The warping, which has four-fold rotational symmetry about the cylinder axis, has been greatly exaggerated for the sake of clarity. The thick curved line represents a closed quasiparticle orbit about the surface caused by the application of a magnetic field **B** parallel to the cylinder axis. The quasiparticle group velocity is normal to the Fermi surface at every point on the orbit. Thus, the warping gives rise to small velocity components parallel to the cylinder axis. (b) Time dependence of the *c* component of the quasiparticle group velocity corresponding to the orbit in (a). The four-fold symmetric warping gives rise to a *c*-axis periodicity which is one quarter of the cyclotron period, i.e. a fourth harmonic of the cyclotron frequency.

Recent angle dependent de Haas–van Alphen (dHvA) measurements by Bergemann et al., have gone a long way towards resolving the precise FS topography of Sr_2RuO_4 [12]. In this paper, we outline a novel complimentary technique based entirely on the semiclassical motion of quasiparticles belonging to the three Sr_2RuO_4 FSs [13]. This effect, which is closely related to cyclotron resonance (first considered by Osada et al. [14], and subsequently by others [13,15]), essentially corresponds to high frequency ($\sim$cyclotron frequency, ω_c) AMRO. The periodic reciprocal space motion (over the FS), induced by the application of a magnetic field, translates into periodic modulations of the real space quasiparticle group velocities ($\perp$FS) as they orbit the warped FSs in a plane perpendicular to the applied field (see Fig. 1a) [13]. This results not only in cyclotron resonance, i.e. essentially 2D orbits within the highly conducting *ab*-planes (as expected for a perfect 2D conductor), but also to an oscillatory *c*-axis motion caused by the FS warping, as depicted in Fig. 1b. Using microwave techniques, one can effectively couple to these *c*-axis velocity oscillations, resulting in so-called periodic orbit resonances (POR) [13]. Harmonic POR series are expected, corresponding to the harmonic content of the FS warping. Thus, GHz AMRO offer an independent means for extracting minute, albeit essential, details of the FS topographies of low-dimensional conductors.

Our preliminary microwave investigations of Sr_2RuO_4 revealed the existence of three series of electron magnetic resonances (both cyclotron resonances and POR), corresponding to the known α, β, and γ bands [16]. More recently, we have examined the angle dependence of these resonances, as well as confirming the precise mechanism by which electromagnetic radiation couples to the oscillatory quasiparticle velocities.

2. Experimental

Several different single crystals of Sr_2RuO_4, of approximate dimensions 2 mm $\times$ 1 mm $\times$ 0.05 mm, were used in this study; all of the samples were grown in the same batch by the method

described in Ref. [17]. Although we did not directly measure the DC conductivity for the samples used in this study, we can estimate an in-plane value of $\sigma_{\parallel} \approx 10^9\ \Omega^{-1}\,\mathrm{cm}^{-1}$ at 2 K, based on the known correlation between T_c (mid-point = 1.44 K for these samples) and the residual low-temperature resistivity [18]. This value, which is comparable to the highest purity copper, implies a mean free path $l \approx 1$ μm, and a penetration depth for in-plane currents ($\delta_{\parallel}$) at 50 GHz of less than 0.15 μm. From the known conductivity anisotropy (≈1500), we estimate a penetration depth for c-axis currents on the order of $\delta_{\perp} \approx 5$ μm.

Measurements were performed using a cavity perturbation technique covering the frequency range from 44 to 112 GHz; for experimental details see Ref. [19]. A single sample was placed in one of two locations within a cylindrical cavity such that either purely in-plane, or a combination of in-plane and interlayer currents were excited via the oscillatory microwave magnetic fields within the cavity (Fig. 2). Due to the small penetration depths, dissipation within the cavity is governed by the surface resistance (R_s) of the sample which, in turn, depends on the precise geometry of the experiment (see Section 3). The sample was oriented with respect to the applied DC magnetic field using a series of sapphire wedges; the sample orientation was subsequently verified using the frequency of Shubnikov–de Haas oscillations which were observed in R_s for all angles for the α FS. Steady magnetic fields were provided by a 33 T resistive magnet at the National High Magnetic Field Laboratory in Tallahassee, FL. Temperature control was achieved via the combination of a resistive heater and a Cernox thermometer attached to the copper cavity containing the sample.

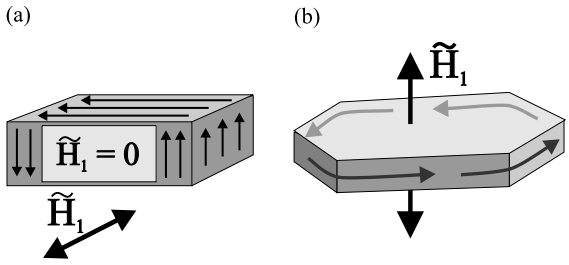

Fig. 2. Circulating currents induced via the oscillatory component of the microwave $\tilde{\mathbf{H}}_1$ fields within the cavity. In (a), the microwave $\tilde{\mathbf{H}}_1$ field is polarized parallel to the ab-plane, thereby inducing both in-plane and interlayer surface currents. In (b) the microwave $\tilde{\mathbf{H}}_1$ field is polarized parallel to the c-axis, thereby inducing only ab-plane currents.

3. Results and discussion

Fig. 3 shows raw data obtained at two different frequencies (76 and 102 GHz), and for two different samples; the data have been scaled so that the horizontal axis corresponds to effective mass ($e\mathbf{B}/\omega m_e$), where $\mathbf{B}$ is the applied field strength and $\omega/2\pi$ is the measurement frequency. For both measurements, the samples were situated within the cavity so that AC currents flow as depicted in Fig. 2a, and such that the DC magnetic field was oriented parallel to the sample c-axis. For this geometry, the average power dissipation $\langle P \rangle$ within the cavity is given by

$$\langle P \rangle = \langle I^2 \rangle \oint R_s \, \mathrm{d}a \tag{1}$$

where $\langle I^2 \rangle$ is the integrated time averaged squared current flowing around the sample; a quasistatic

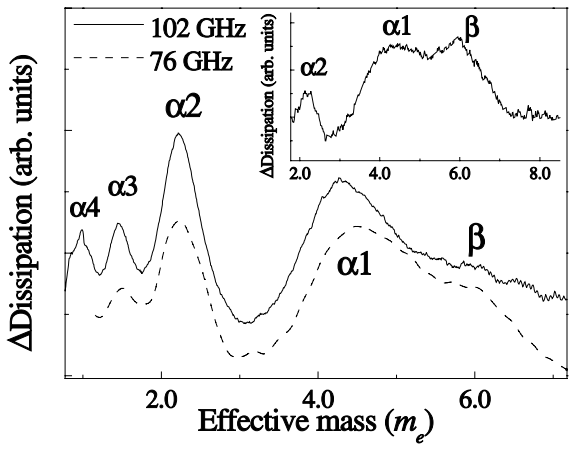

Fig. 3. Resonant absorptions as a function of scaled magnetic field in units of effective mass ($= e\mathbf{B}/\omega m_e$, see text); the temperature was 1.5 K in each case. The data in the main part of the figure was obtained for the experimental configuration shown in Fig. 2a, while the inset shows data obtained at 76 GHz for the experimental configuration shown in Fig. 2b.

approximation allows us to remove this quantity from the integral, i.e. the integrated current flowing across each surface at any time must be the same [20]. Thus the relative contribution of each surface to the dissipation is given simply by the product of that surface's area and its surface resistance [20]. For the geometry depicted in Fig. 2a, in-plane currents flow across the large flat surfaces (denoted $\|$), while interlayer currents complete the circuit at the short edges (denoted $\perp$) of the sample. Surface resistance is proportional to penetration depth, thus, the ratio of the appropriate surface resistances for the $\perp$ and $\|$ surfaces is given by $\delta_\perp/\delta_\| \approx 33$. Meanwhile, the ratio of the surface areas ($A_\|/A_\perp$) for the samples used in this study range from between 20 and 50. Consequently, these two factors approximately cancel, and one can expect in-plane and interlayer currents to contribute more or less equally to the dissipation for this experimental geometry.

We are now in a position to understand the different resonant peaks observed in Fig. 3. Each of the peaks observed below $\approx 3m_e$ is harmonically related to the peak centered at around $4.35m_e$; these peaks are labeled $\alpha 1$, $\alpha 2$, etc., corresponding to the first, second, etc., harmonics of the cyclotron mass due to the α FS. These assignments are based on our original studies in Ref. [16]. For an approximately 2D tight-binding band, one expects to observe only odd cyclotron harmonics in the in-plane conductivity, which diminish in weight with increasing harmonic index [21]. Consequently, the strong second harmonic (stronger than fundamental), and the fourth harmonic seen in the 102 GHz data, must be due to interlayer currents, i.e. POR. Indeed, these harmonics are expected on the basis of the studies by Bergemann et al., which predict significant two-fold and four-fold warping components to the α FS [12]. These components contribute to a sizeable fraction ($\approx$20–30%) of the interlayer conductivity and should, therefore, exhibit strong PORs at the second and fourth harmonics of the fundamental cyclotron resonance. The fact that the relative strengths of the first and second harmonics differ by about 25% for the two samples studied may be attributable to the different sample shapes, i.e. different relative contributions from in-plane and interlayer currents. The appearance of a third harmonic is consistent with the predicted diamond shaped cross-section of the α FS [16].

The inset to Fig. 3 shows data obtained at 76 GHz for a geometry such that predominantly in-plane currents are excited, as depicted in Fig. 2b; the DC field is again applied parallel to the c-axis. For this configuration, the high harmonic content to the α resonance has diminished considerably. The weak remnant $\alpha 2$ peak is probably due to the large sample size, which causes part of the sample to extend into regions of the cavity that cause interlayer current excitation. Alternatively, $\alpha 2$ is close to the location where $\beta 3$ would be expected – β being the heavier effective mass resonance due to the β FS (see below) – though the shape of the β FS is not expected to produce a significant $\beta 3$ component to the in-plane cyclotron resonance [16]. We note here that, although the experimental geometry used here is suitable for observation of Azbel–Kaner cyclotron resonance (+ harmonics), the appropriate penetration depth would be $\delta_\perp \approx$ 5μm which is considerably greater than the cyclotron radius (<1 μm) in this magnetic field range [22].

Next we turn to the angle dependence of the resonances. Ideally, one would like to rotate the cavity with respect to the DC field, thus leaving the electromagnetic coupling between the sample and the AC microwave fields unchanged. However, the extremely high sensitivity cylindrical cavities used in this study do not permit such mechanical adjustments within the restricted confines of the high field magnets at Tallahassee [19]. Consequently, there is greater uncertainty as to the exact nature of the induced current flow for these measurements. Fig. 4 shows data obtained at two frequencies with the DC field applied at an angle $\theta = 45°$ away from the c-axis. Resonances corresponding to β, α and $\alpha 2$ are observed; again, these assignments agree excellently with our earlier studies [16]. In addition, these resonances move to higher magnetic field upon increasing the frequency, as expected for cyclotron-like resonances. Like the data in the inset to Fig. 3, the $\alpha 2$ resonance is quite weak in comparison to α, implying that dissipation is dominated by in-plane currents. The γ resonance is beyond the attainable field

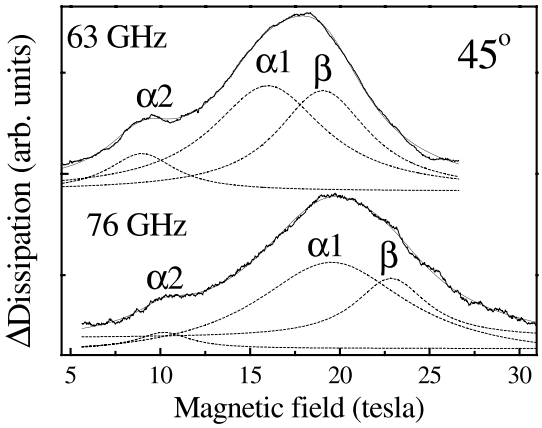

Fig. 4. Data obtained at two frequencies with the magnetic field tilted 45° away from the c-axis; the temperature was 1.5 K in each case. The dashed lines show the individual contributions to the resonances obtained from a Lorentzian fitting procedure.

range for this angle and at these relatively high frequencies.

Finally, in Fig. 5 we compile data obtained for three different angles θ between the applied DC magnetic field and the sample c-axis. The data have been scaled to $\theta = 0°$ by dividing the resonance fields by $\cos\theta$, as expected for weakly warped quasi-two-dimensional FS cylinders. By plotting the scaled resonance fields versus frequency in this way, the data accumulate on one of several straight lines passing through the origin, each line corresponding to a different cyclotron effective mass (or a harmonic). The effective masses obtained from this analysis agree to within less than 1% with the values deduced from our earlier study [16], i.e. $m_\alpha = 4.30m_e$, $m_\beta = 5.76m_e$, and $m_\gamma = 9.73m_e$. These values are considerably lower than those obtained from dHvA measurements [23] – this difference is attributable to many body effects, as discussed in Ref. [16]. The $1/\cos\theta$ scaling provides further conclusive proof that the resonances do originate from closed cyclotronic reciprocal space orbits of quasiparticles about the approximately cylindrical α, β, and γ FSs.

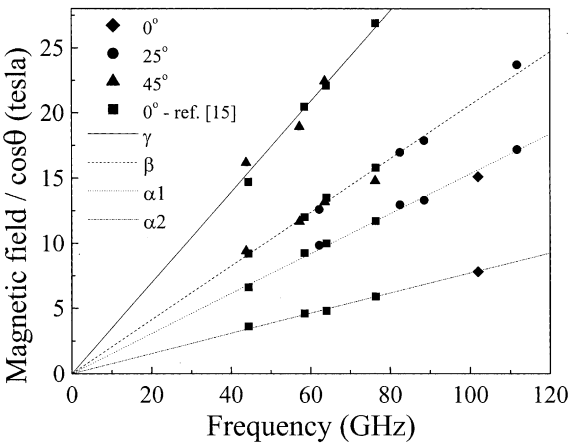

Fig. 5. A compilation of all of the resonance positions (scaled to $\theta = 0°$) as a function of frequency. The straight lines correspond to fits to each series of resonances, from which effective masses are extracted.

4. Summary and conclusion

We have observed cyclotron resonances and POR in the triplet superconductor Sr_2RuO_4. From the angle dependence, which was lacking in the previous study, we confirm the two-dimensional character of these resonances. Furthermore, by performing measurements on several samples in different electromagnetic field configurations, we are able to couple to different cyclotron modes (+ harmonics) which derive from deformations (warpings) of the Fermi surfaces from perfect cylinders, thereby confirming our originally proposed mechanism for resonant absorption. Our findings also appear to be in excellent agreement with recent angle dependent dHvA measurements.

Acknowledgements

This work was supported by NSF-DMR 0071953, the Office of Naval Research (N00014-98-1-0538) and Research Corporation. Work carried out at the NHMFL was supported by a cooperative agreement between the State of Florida and the NSF under DMR-95-27035.

References

[1] A.P. Mackenzie, Y. Maeno, Physica B 280 (2000) 148.
[2] D. Vollhardt, P. Wolfe, The Superfluid Phases of Helium 3, Taylor and Francis, London, 1990.

[3] K. Ishida, H. Mukuda, Y. Kitaoka, Z.Q. Mao, Y. Mori, Y. Maeno, Phys. Rev. Lett. 84 (2000) 5387 and references therein.
[4] G.M. Luke, Y. Fudamoto, K.M. Kojima, M.I. Larkin, G. Merrin, B. Nachumi, Y.J. Uemura, Y. Maeno, Z.Q. Mao, Y. Mori, H. Nakamura, M. Sigrist, Nature 394 (1998) 558.
[5] Y. Sidis, M. Braden, P. Bourges, B. Hennion, S. NishiZaki, Y. Maeno, Y. Mori, Phys. Rev. Lett. 83 (1999) 3320.
[6] D.J. Scalapino, Phys. Rep. 250 (1995) 329.
[7] T. Kuwabara, M. Ogata, Phys. Rev. Lett. 85 (2000) 4586.
[8] T. Takimoto, Phys. Rev. B 62 (2000) R14641.
[9] E. Ohmichi, H. Adachi, Y. Mori, Y. Maeno, T. Ishiguro, T. Oguchi, Phys. Rev. B 59 (1999) 7263.
[10] A. Damascelli, D.H. Lu, K.M. Shen, N.P. Armitage, F. Ronning, D.L. Feng, C. Kim, Z.-X. Shen, T. Kimura, Y. Tokura, Z.Q. Mao, Y. Maeno, Phys. Rev. Lett. 85 (2000) 5194.
[11] I.I. Mazin, D.A. Papaconstantopoulos, D.J. Singh, Phys. Rev. B 61 (2000) 5223 and references therein.
[12] C. Bergemann, S.R. Julian, A.P. Mackenzie, S. Nishizaki, Y. Maeno, Phys. Rev. Lett. 84 (2000) 2662.
[13] S. Hill, Phys. Rev. B 55 (1997) 4931.
[14] T. Osada, S. Kagoshima, N. Miura, Phys. Rev. B 46 (1992) 1812.
[15] A. Ardavan, J.M. Schrama, S.J. Blundell, J. Singleton, W. Hayes, M. Kurmoo, P. Day, P. Goy, Phys. Rev. Lett. 81 (1998) 713.
[16] S. Hill, J.S. Brooks, Z.Q. Mao, Y. Maeno, Phys. Rev. Lett. 84 (2000) 3374.
[17] Y. Maeno, J. Phys. Soc. Jpn. 66 (1997) 1405.
[18] A.P. Mackenzie, R.K.W. Haselwimmer, A.W. Tyler, G.G. Lonzarich, Y. Mori, S. Nishizaki, Y. Maeno, Phys. Rev. Lett. 80 (1998) 161.
[19] M. Mola, S. Hill, P. Goy, M. Gross, Rev. Sci. Inst. 71 (2000) 186.
[20] S. Hill, Phys. Rev. B 62 (2000) 8699.
[21] S.J. Blundell, A. Ardavan, J. Singleton, Phys. Rev. B. 55 (1997) 6129.
[22] A.A. Abrikosov, Fundamentals of the Theory of Metals, Elsevier, Amsterdam, 1988.
[23] A.P. Mackenzie, S.R. Julian, A.J. Driver, G.J. McMullan, M.P. Ray, G.G. Lonzarich, Y. Maeno, S. Nishizaki, T. Fujita, Phys. Rev. Lett. 76 (1996) 3786.